# Rare Earth Superlattices

D. F. McMorrow

Department of Solid State Physics, Risø National Laboratory,

DK-4000 Roskilde, Denmark

## Abstract

A review is given of recent experiments on the magnetism of rare earth superlattices. Early experiments in this field were concerned mainly with systems formed by combining a magnetic and a non-magnetic element in a superlattice structure. From results gathered on a variety of systems it has been established that the propagation of magnetic order through the non-magnetic spacer can be understood mostly on the basis of an RKKY-like model, where the strength and range of the coupling depends on the details of the conduction electron susceptibility of the spacer. Recent experiments on more complex systems indicate that this model does not provide a complete description. Examples include superlattices where the constituents can either be both magnetic, adopt different crystal structures (Fermi surfaces), or where one of the constituents has a non-magnetic singlet ground state. The results from such systems are presented and discussed in the context of the currently accepted model.

## 1 Introduction

The first rare earth superlattices were produced by molecular beam epitaxy (MBE) a little over a decade ago. The initial results from these systems had an immediate impact on the field of magnetism in metals, in that they provided a new window on the nature of the magnetic coupling in the metallic state. This early work also helped to stimulate studies of transition metal superlattices, which eventually resulted in the discovery of the giant magneto-resistance effect (Baibich et al., 1988).

Two of the key early papers in the field of rare earth superlattices were both concerned with the magnetism of a system formed from a magnetic element interleaved with a Y spacer block. (Y is an almost ideal element for these studies as it has the hcp structure and is well latticed matched ($\approx 2\%$) with the heavy rare earths.) The idea behind these experiments was to investigate how the magnetic order is transmitted through the spacer block. In the case of Dy/Y it was discovered by Salamon et al. (1986) that the helical order adopted by the Dy $4f$ moments propagates coherently through the Y block. A natural explanation for

this observation was an RKKY-like coupling between the Dy blocks through the Y (see, for example, Yafet et al., 1988). Although Y is itself non-magnetic it does have a large peak in its conduction susceptibility, $\chi(\mathbf{q})$, at about the same position as the ordering wave vector in Dy (Liu et al., 1971). Thus, when the $4f$ moments in the Dy block order, they spin polarize the conduction band of the Y to form a spin-density wave, and it is this spin-density wave that carries information on the order from one magnetic block to the next. In this view, the range over which the order can be propagated coherently (the magnetic coherence length) is determined by the width and height of the peak in the conduction susceptibility of the spacer layer. A second important result of this work was that the helical-to-ferromagnetic transition of bulk Dy is suppressed in the superlattice. This was shown to be a consequence of the clamping of the Dy blocks by the Y. At about the same time as the work on Dy/Y was published, Majkrzak et al. (1986) reported the results of an investigation of Gd/Y. For this system it was found that the Gd within an individual block ordered ferromagnetically (as in the bulk), and that the coupling between successive blocks of Gd oscillated between being ferro- or antiferromagnetic depending on the thickness of the Y spacer. The period of the oscillation was also found to be consistent with that expected on the basis of an RKKY-like coupling.

The study of rare earth superlattices has continued to develop, with several dedicated MBE plants around the world now producing samples, but with a change of emphasis to investigate more complex systems, such as fabricating superlattices from two magnetic elements. All of the examples presented here result from a collaboration between the Clarendon Laboratory and Risø National Laboratory. For more comprehensive accounts of the work on rare earth superlattices the reader is referred to the reviews by Majkrzak et al. (1991), and Rhyne et al. (1993). The development of this subject has relied extensively on neutron scattering results, and this is reflected in this review, where all of the examples given have used this technique.

## 2   Sample growth

The samples of interest here are all produced using MBE techniques, and a schematic of a superlattice is shown in Fig. 1. In MBE the material to be grown is evaporated from a source (usually a crucible that is heated in some way) so that it is deposited on a substrate, with an evaporation rate that allows for the control of the growth down to the sub-monolayer level. The main requirements for the production of good quality superlattices, with flat interfaces between the constituents, are that the substrate must be atomically flat, there must be as close a match as possible
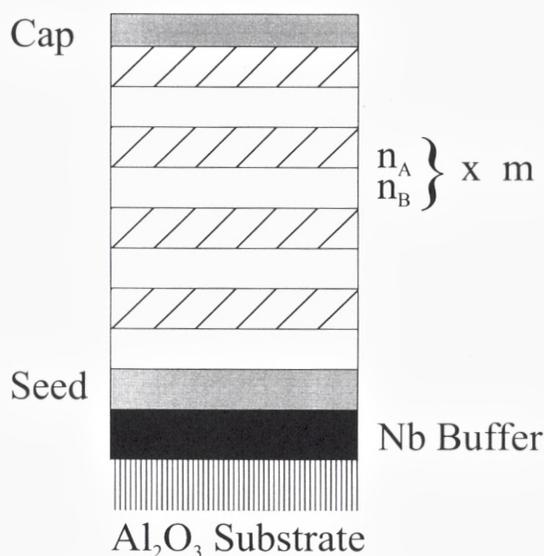
Figure 1. A schematic of the structure of a rare earth superlattice. For all of the superlattices of interest here the growth direction is parallel to the $c$ axis of the rare earth metal. Each superlattice unit cell is made up from $n_A$ atomic planes of element $A$ and $n_B$ planes of element $B$, with the unit cell repeated m times, so that the complete superlattice can be designated as $(A_{n_A}/B_{n_B})_m$. The seed layer is normally one of the non-magnetic elements Y, Lu or Sc.

between the lattice parameters of the substrate and the deposited material, and they should not react chemically. These requirements are often difficult to realize in practice, and the rather elaborate foundation of the superlattice shown in Fig. 1 is the best solution that has been found to date for the rare earths (Kwo et al., 1985, 1987). In fact the mosaic spread of the completed superlattice can be as little as $\approx 0.15°$, which is low compared to typical values for bulk crystals of the rare earths, and from this point of view the superlattices may be regarded as good single crystals. X-ray diffraction experiments also show that the interfaces are well defined, with interdiffusion limited to approximately four atomic planes (McMorrow et al., 1996, and references therein).

In what follows we shall refer to the superlattice unit cell as a bilayer, which is composed of $n_A$ atomic planes of element $A$ and $n_B$ atomic planes of element $B$. This bilayer unit is then repeated $m$ times, so that the superlattice may be written as $(A_{n_A}/B_{n_B})_m$. Values for $n$ are chosen to lie in the range of 5 to 50, while $m$ is usually around 100 or fewer. This means that the superlattice is at best 1 $\mu$m thick, and for a 1 cm$^2$ substrate there is less than one 1 milligram of sample.

# 3   Magnetism in a system with a large lattice mis-match: Ho/Sc superlattices

In addition to using either Y there is also the possibility of exploring what happens when other non-magnetic elements are used to form the spacer layer. Several systems have been grown with Lu as the spacer, and these include Dy/Lu (Beach et al., 1992), Ho/Lu (Swaddling et al., 1993, 1996). Sc is another obvious choice as it also adopts the hcp structure, while band structure calculations (Lui et al., 1971) suggest that it has a peak in its conduction electron susceptibility qualitatively similar to that in Y, albeit weaker and broader. The main problem in using Sc, however, is that it has lattice parameters that are approximately 7% smaller than those of the heavy rare earths such as Ho. In spite of this it proved possible to produce superlattices of Dy/Sc (Tsui et al., 1993), which did not display any long-range magnetic order, but had instead short-range ferromagnetic correlations at temperatures well above $T_C$ of bulk Dy. More recently Bryn-Jacobsen et al. (1997) have studied a series of Ho/Sc superlattices, which display a number of interesting structural and magnetic properties.

We shall first consider their structural properties. When attempting to produce a superlattice from two constituents that have a lattice mis-match, it may occur that the mis-match is so large that the lattice parameters of the individual blocks within the superlattice relax back to their bulk values. This occurs if the critical thickness for the formation of misfit dislocations is comparable to or smaller than the desired thickness of the block. Its signature is the appearance of two distinct peaks in a scan of the wave vector in the plane of the film, one for each of the constituents. Using a combination of x-ray and neutron scattering techniques, Bryn-Jacobsen et al. (1997) established that this was indeed the situation for Ho/Sc, as shown schematically in Fig. 2. (For other systems studied, where the lattice mismatch is smaller, only a single peak representative of the average lattice parameter has been found.) Thus, Ho/Sc superlattices are essentially composed of blocks of Ho and Sc with almost their respective bulk lattice parameters. While there is a strong correlation in the the position of the close packed planes from block to block, the hcp stacking sequence (ABAB···) is not maintained from one block to the next.

These unusual structural features also express themselves when we come to consider the magnetic structure. In Fig. 3 two scans are shown with the wave vector transfer **Q** scanned parallel to the $c^*$ direction for a $Ho_{30}/Sc_{10}$ superlattice. In the top panel the scan direction is $[00\ell]$. Around the position of the (002) Bragg peak (in the range 2.2 to 2.35 $Å^{-1}$) sharp satellite peaks are evident. These arise from the contrast in the nuclear scattering lengths of Ho and Sc. Symmetrically

X

(002) ●

X

<br>

X  ●  ● (101)

●

[001]                    X

↑

└→

●  ●  ● (100)
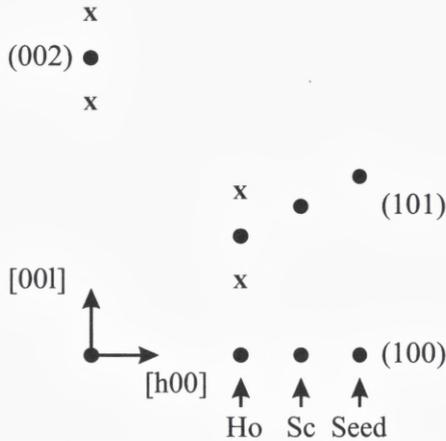
[h00]  ↑  ↑  ↑

Ho  Sc  Seed

Figure 2. A schematic (not to scale) of the reciprocal space in the $(h0\ell)$ plane of Ho/Sc superlattices. Filled circles represent nuclear Bragg peaks from the hcp lattice, while crosses indicate regions where magnetic scattering would be detected for a helical arrangement of the moments. (For clarity the positions of the magnetic satellites around the origin are not shown.) The width of the scans for $\mathbf{Q}$ along $[00\ell]$ is a measure of the coherence in the stacking of the close-packed planes. Scans of $\mathbf{Q}$ along $[h00]$ reveal the existence of more than one $a$ lattice parameter (Bryn-Jacobsen et al., 1997).

displaced either side of the (002) peak is the magnetic scattering, which is only seen when the sample is cooled below $\approx 132$ K, the bulk ordering temperature of Ho (Koehler et al., 1966), and which indicates that the Ho moments within an individual Ho block form a helix. In contrast to the nuclear scattering, the magnetic scattering is extremely broad, showing that the magnetic correlations are short-ranged. In fact the magnetic correlations just extend between nearest-neighbour blocks of Ho ($\approx 150$ Å for this sample). One of the unusual aspects of the magnetic structure, deduced from fits to the scattering data by Bryn-Jacobsen et al. (1997), is that while individual Ho blocks are helically ordered, the coupling between blocks is antiferromagnetic. Whether this results from the effect of a dipolar coupling, or from some other type of coupling has yet to be established.

In the bottom panel of Fig. 3 the scan direction is $[10\ell]$ (see Fig. 2) through the position of the $(101)_{\mathrm{Ho}}$ peak. (The Ho subscript refers to the fact that the value of $h$ was set for the position of the (100) for the Ho blocks.) As this scan direction has a component $\mathbf{Q}$ in the basal plane, it is sensitive to the stacking sequence of the hcp planes. As the scattering at the position of $(101)_{\mathrm{Ho}}$ is broad, it is clear that this stacking sequence is disordered. This is also reflected in the magnetic scattering at $(1\,0\,1-q)_{\mathrm{Ho}}$ and $(1\,0\,1+q)_{\mathrm{Ho}}$, which is well described by a broad Gaussian line
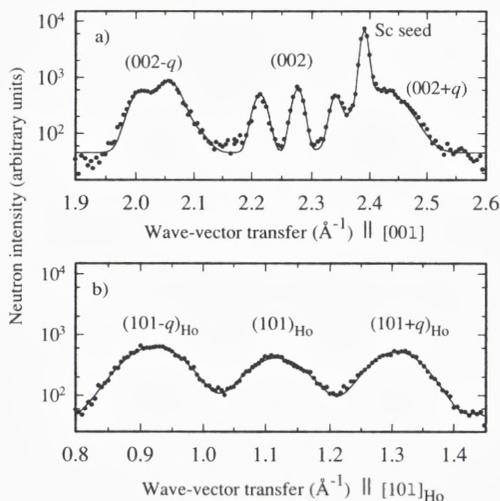
Figure 3. The neutron scattering observed at 4 K from $Ho_{30}/Sc_{10}$. (a) A scan of **Q** along $[00\ell]$ showing nuclear superlattice peaks around (002). The peaks at positions $(002\pm q)$ are magnetic in origin, and can be identified with helical ordering of the Ho moments. (b) A scan along $[10\ell]_{Ho}$ with an absence of any nuclear superlattice peaks around $(101)_{Ho}$. The peaks at positions $(101\pm q)_{Ho}$ arise from a helical configuration of the moments (Bryn-Jacobsen et al., 1997).

shape.

It is also instructive to compare the systematic dependence of the magnetism as the spacer material is varied. Perhaps the parameter that is most readily obtained from a scattering experiment, and one that does not depend on any modelling of the structure, is the magnetic coherence length, $\zeta$. Here $\zeta$ is defined by $\zeta = 2\pi/\Delta Q$, where $\Delta Q$ is the width (FWHM) of the magnetic peak. The results for the Ho/X series, with X = Y, Lu or Sc are collected in Fig. 4. For the cases of Y and Lu it can be seen that the coherence length is as large as 1000 Å for spacer layers below about 10 atomic planes, and that it decreases rapidly (roughly as $1/r$) as the spacer thickness is increased. There is a marked tendency for the magnetic coherence to persist to greater distances in Y-based systems than those with Lu. In contrast, the Sc-based systems exhibit short-range order for all thicknesses of Sc investigated. These results may be considered to be in qualitative agreement with what is expected on the basis of an RKKY model of the coupling, and the known properties of the conduction electron susceptibilities $\chi(\mathbf{q})$ of the spacer layer, either derived from calculations or experiments. The calculations of Liu et al. (1971) show that the for the three spacer elements considered here, the peak in $\chi(\mathbf{q})$ is strongest
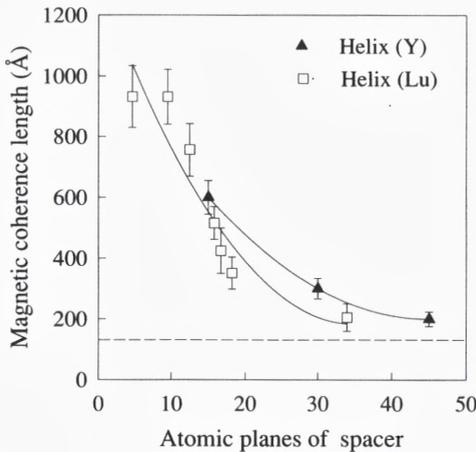
Figure 4. A comparison of the dependence of the magnetic correlation length as a function of the spacer layer thickness for Ho/X superlattices, where X = Y (Jehan et al., 1993), Lu (Swaddling et al., 1996) or Sc (Bryn-Jacobsen et al., 1997). The solid lines are guides for the eye, whereas the dotted line represents an average of the results for Sc.

and sharpest for Y, and is weaker, and possibly broader, for Sc and Lu. The peak in $\chi(\mathbf{q})$ for Sc is, however, predicted to be similar to that of Lu, and so it is not immediately clear why the coherence length in the former is so small. It could well be that another factor, such as an enhanced scattering of the conduction electrons from the greater concentration of defects in the Sc based systems plays a part in limiting the development of long-range order. More accurate calculations of $\chi(\mathbf{q})$ for these elements would be of obvious use in trying to resolve this question.

# 4   Persistence of helical order in Dy/Ho superlattices

As a first example of a system fabricated from two magnetic rare earths, we will consider the Dy/Ho system studied by Simpson et al. (1996) using time-of-flight neutron diffraction. This work is of interest as it illustrates how simple ideas based on modifications of the magnetic structure through strain can be misleading.

Previous studies of Dy-based superlattices include Dy/Y (Salamon et al., 1987; Erwin et al., 1987) and Dy/Lu (Beach et al., 1992), where very different behaviour was found for the temperature dependence of the turn angle $\psi_{\mathrm{Dy}}$ in the Dy blocks. Due to the lattice mis-match between the Dy and spacer blocks, in the former there

is an expansive basal-plane strain of the Dy, which results in the ferromagnetic phase found below $T_C = 78$ K in bulk Dy being suppressed at all temperatures. In contrast, there is a compressive strain for the Dy blocks in Dy/Lu, and $T_C$ is slightly enhanced. The strain for the Dy layers in Dy/Ho is the same sign as that for Dy/Lu, although the lattice mis-match is much smaller: 0.4% compared to 2.5%. If strain alone was the sole factor in determining the modification of the magnetic structure of Dy in a superlattice, then it would be expected that the Dy in Dy/Ho would have a slightly higher $T_C$ than the bulk.

Two superlattices of Dy/Ho were studied of composition $Dy_{32}/Ho_{11}$ and $Dy_{16}$ /$Ho_{22}$. Both samples studied were found to order magnetically at a temperature consistent with that of bulk Dy (179 K) (Wilkinson et al., 1961). From this temperature down to approximately the bulk ordering temperature of Ho, a good description of the scattering was obtained by assuming that the $4f$ moments in the Dy blocks formed a helix, while those in the Ho blocks remained paramagnetic. Moreover, the coupling of the Dy through the disordered Ho was long range, with an effective turn angle per layer through the Ho that was essentially the same as that found in bulk Ho at its ordering temperature. As the temperature was lowered below $T_C$ of Dy no dramatic change in the scattering was noted. In particular the intensity of the (002) peak did not increase on cooling through $T_C$, as would be expected if the Dy moments collapsed into a basal-plane ferromagnet. A representative scan below $T_C$ is shown in Fig. 5. Here it is evident that the scattering is qualitatively consistent with that expected from a system in which there is helical order in both components of the superlattice; the superlattice sub-structure in the magnetic (M) peaks results from the fact that the magnitude of the ordered moment in the Dy and Ho blocks is not identical.

The results of fitting the data to extract the individual turn angles (or equivalent wave vectors) are summarised in Fig. 6, where they are compared to the behaviour of the bulk. For the case of Dy, it can be seen that above $T_C$, the wave vector of the Dy blocks in the superlattice is slightly higher than that in the bulk, and that below $T_C$ it appears to lock in to a value of $(1/6)c^*$. The wave vector in Ho is essentially independent of temperature above $T_N(\text{Ho})$, and then decreases below this temperature.

The fact that the Dy remains in a helical phase at all temperatures below $T_N(\text{Dy})$ in Dy/Ho superlattices is clearly at variance with what would have been predicted if the system was considered to be isolated, but strained, blocks of Dy and Ho. This indicates that the magnetic structure assumed by the Dy must depend on the magnetic structure of the superlattice taken as a whole. The reduction in energy from the formation of a coherent helical structure in both materials, without the disruption that would occur at the interface if the Dy were ferromagnetic, must then more than offset the energy cost of Dy remaining helical.
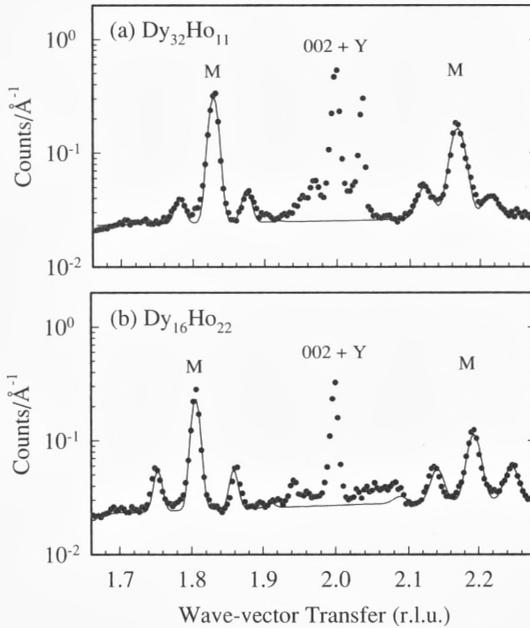
Figure 5. The neutron scattering with the wave-vector transfer along [00$\ell$] observed at $T = 40$ K from (a) $Dy_{32}/Ho_{11}$ and (b) $Dy_{16}/Ho_{22}$. The solid line is a fit to the data of a model with basal-plane helical ordering of both the Dy and Ho moments. The peaks near $Q = 2c^*$ are the (002) nuclear Bragg peaks and are not included in the model of the magnetic structure. M indicates the position of the main magnetic satellites, each of which is seen to have its own superlattice side peaks. (Simpson et al., 1996).

We also not that interesting results have also been reported recently for other superlattices containing two magnetic elements, including Ho/Er (Simpson et al., 1994) and Dy/Er (Dumensil et al., 1994).

# 5    Magnetism in a mixed hcp/dhcp superlattice

So far we have restricted ourselves to a consideration of the heavy rare earths only. For the present considerations, there are two salient features of the light rare earths compared to the heavies: they have more complex crystal structures, and the nesting features of the Fermi surface may be such that $\chi(\mathbf{q})$ is peaked at
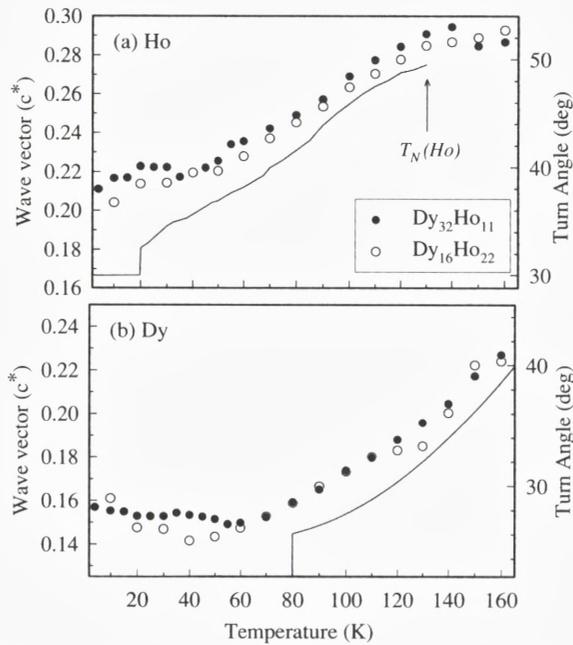
Figure 6. The wave vector (and equivalent turn angle) for (a) Ho and (b) Dy moments deduced from the model described in the text ($\circ$ Dy$_{16}$/Ho$_{22}$; $\bullet$ Dy$_{32}$/Ho$_{11}$). The variation of the bulk value for each element is shown by the solid lines. (Simpson et al., 1996).

finite $\mathbf{q}$ along $a^*$, instead of along $c^*$ as found in the heavy rare earths. By way of example, Nd and Pr both adopt the dhcp structure, and order magnetically with a propagation wave vector within the hexagonal basal planes (Jensen and Mackintosh, 1991). The motivation in producing a mixed hcp/dhcp superlattice is then to determine its structural and magnetic properties. In particular, it is interest to study the consequences of the mis-match in the Fermi surfaces [or equivalently the mis-match in $\chi(\mathbf{q})$] on the propagation of magnetic order.

As far as we are aware, there have been only two reports of work on mixed hcp/dhcp superlattices: Nd/Y by Everitt et al. (1995), and Ho/Pr by Simpson et al. (1995). In total three different superlattices were investigated by Simpson et al. (1995), with nominal compositions of Ho$_{20}$/Pr$_{20}$, Ho$_{30}$/Pr$_{10}$, and Ho$_{24}$/Pr$_6$. From scans of $\mathbf{Q}$ performed along the $[10\ell]$ direction at room temperature it was deduced that the Pr blocks in the superlattice retain their dhcp stacking (ABAC$\cdots$), but as might be expected, the dhcp stacking was not coherent from one Pr block to the next.
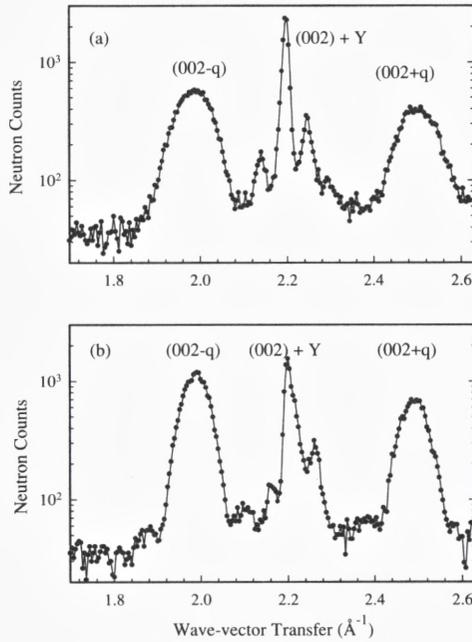
Figure 7. The neutron scattering observed at 10 K with the wave-vector transfer along [$00\ell$] for (a) the $Ho_{20}/Pr_{20}$ and (b) $Ho_{30}/Pr_{10}$. The broad magnetic peaks occur at $q$ from the nuclear peaks and indicate short-range helical magnetic order in the Ho blocks (Simpson et al., 1995).

The key results relating to the magnetic structure of the Ho/Pr superlattices are summarised in Fig. 7. This shows the scattering at 10 K from the $Ho_{20}/Pr_{20}$ (top panel) and $Ho_{30}/Pr_{10}$ (bottom panel) superlattices when **Q** was scanned along the [$00\ell$] direction through the (002). As with the previous examples of Ho-based superlattices in Sect. 3 and Sect. 4, the gross features of the magnetic scattering is consistent with those expected from a basal-plane helix: there are magnetic peaks displaced $\pm q$ from the (002) nuclear peak. The (002) has sharp superlattice peaks, reflecting the good coherence in the stacking of the close-packed planes. The broad magnetic scattering, however, is well described by a single Gaussian line shape, and the coherence length extracted from its width indicates that the magnetic correlations are completely confined to lie within the individual Ho blocks. In some ways this is reminiscent of the scattering from the Ho/Sc superlattices shown in Fig. 3. The difference, however, is that in that particular case there was a short-range antiferromagnetic coupling between the Ho blocks. For Ho/Pr there

is no coupling between adjacent Ho whatsoever. (We note that the strain in the Ho/Pr system is considerably smaller than in Ho/Sc.) From the neutron scattering it has not proved possible to determine whether or not the Pr ions retain the non-magnetic ground state of the bulk (McEwen and Stirling, 1981; Bjerrum Møller et al., 1982).

Thus, it appears that the effect of the Pr blocks is to completely decouple the magnetic correlations between blocks of Ho. The most plausible explanation for this effect is the differences in the nesting features of the Fermi surfaces of the two constituents, which in Ho produce a peak in $\chi(\mathbf{q})$ along the $c^*$ axis, whereas in Pr it is peaked in the $a^*$ direction. Any conduction-electron-mediated coupling of the Ho blocks along $c$ would then depend on the details of the Pr conduction electron susceptibility along that direction. The calculations by Liu et al. (1971) suggest a ferromagnetic coupling should be favoured in Pr, whereas in fact an antiferromagnetic structure occurs. It seems clear, therefore, that without a better description of $\chi(\mathbf{q})$ for Pr it is difficult to draw any further conclusions.

# 6   Induced magnetic order in Nd/Pr superlattices

The final example is taken from some very recent work on superlattices formed from the two light rare-earths Nd and Pr (Goff et al., 1996). In their bulk form both Pr and Nd adopt the dhcp structure, which has two inequivalent sites in the chemical unit cell of approximately cubic and hexagonal symmetry.

Although Nd and Pr sit next to each other in the periodic table their magnetic properties are very different. The $4f$ moments on the hexagonal sites in bulk Nd order below about 20 K to form an incommensurable structure (Moon et al., 1964). Both the wave vector describing the order and the moments themselves are confined to the basal plane, and hence are perpendicular to $c$, the superlattice modulation direction. Below about 8 K in Nd the cubic sites also order. Pr on the other hand has a non-magnetic singlet groundstate and only orders spontaneously below 0.05 K (McEwen and Stirling, 1981; Bjerrum Møller et al., 1982).

In Fig. 8 results of the scattering from the hexagonal sites of two superlattices of Nd/Pr are compared. The top panel shows the magnetic scattering from $Nd_{33}/Pr_{33}$, where well defined superlattice peaks are evident either side of the main magnetic peak. The width of the individual peaks is a direct measure of the magnetic coherence length and it can be immediately deduced that the magnetic order in the Nd blocks propagates coherently through the Pr to form a long-range structure. The fact that the superlattice peaks are readily observed also shows that there is a large contrast between the size of the magnetic moments in the Nd and Pr blocks. The solid line through the data is the result of a calculation where it
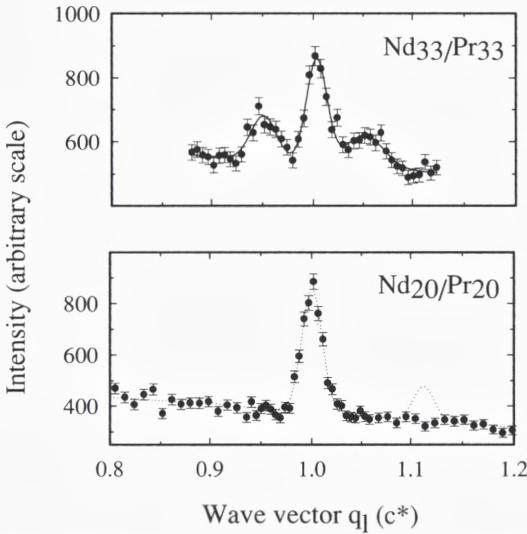
Figure 8. Scans along the $c^*$ direction through the magnetic reflections in Nd/Pr from the hexagonal sites at 10 K from (a) $Nd_{33}/Pr_{33}$ and (b) $Nd_{20}/Pr_{20}$. The solid line in (a) is the result of a calculation assuming that there is no ordering of the $4f$ moments in the Pr, while in (b) a similar calculation is given by the dotted line which does not go through the experimental points. For (a) and (b) the scan direction was along $q_l$ through $(q_h^{hex}\, 0\, q_l)$ with $q_h^{hex} \approx 0.14$ r.l.u. (Goff et al., 1996).

has been assumed that there is a negligible moment in the Pr blocks, as would be expected if the Pr ions retained the non-magnetic singlet groundstate of the bulk. When the thickness of the Pr spacer is reduced a quite different result is obtained, as shown in Fig. 8(b) for $Nd_{20}/Pr_{20}$. Here just a single magnetic peak is observed, even though calculations of the magnetic scattering, performed assuming no ordering of the local moments in the Pr, predict that superlattice substructure should be visible. What in fact is happening in this sample is that the Nd moments have induced the local Pr moments to order so that a uniform magnetic structure is established throughout the superlattice. This is shown more clearly in the top panel of Fig. 9, where the temperature dependence of $\mu_{Pr}/\mu_{Nd}$, the ratio of the Pr to Nd moments, is plotted for $Nd_{20}/Pr_{20}$ and $Nd_{33}/Pr_{33}$. For the former sample with the thinner layers the Pr and Nd moments have, within error, the same magnitude at all temperatures below $T_N$, whereas for the latter the Pr moment is small until the sample is cooled below 6 K. It is worth noting that for the $Nd_{33}/Pr_{33}$ sample this temperature coincides with a marked decrease in the coherence length of the
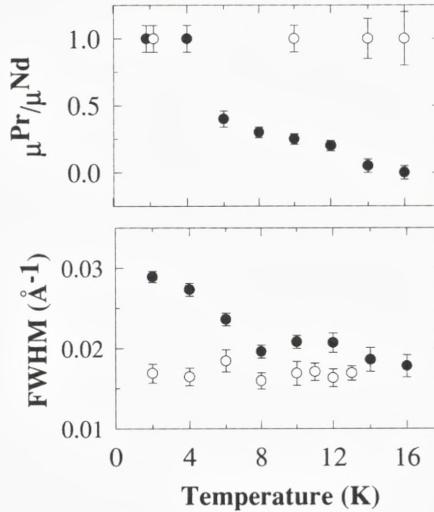
Figure 9. Temperature dependence of (a) the ratio of the Pr to Nd moment and (b) the width of the magnetic reflection along $c^*$ for two Nd/Pr superlattices. Key: o $Nd_{20}/Pr_{20}$, • $Nd_{33}/Pr_{33}$ (Goff et al., 1996).

hexagonal site order (as shown in the lower panel of Fig. 10), and the onset of order on the cubic sites. The cubic sites in $Nd_{20}/Pr_{20}$ were not observed to order for temperatures down to 2 K.

One further interesting feature of the Nd/Pr system is shown in Fig. 10. For the same $Nd_{33}/Pr_{33}$ superlattice that displayed coherent magnetic order on the hexagonal sites, the order on the cubic sites is short range (as attested to by the very broad peak) and restricted to a single block of Nd.

# 7   Summary

The examples in this review have been chosen to illustrate current trends in the study of rare earth superlattices. It is has been emphasised that while the coupling mechanism that determines the magnetic structures undoubtedly has many of the features associated with an RKKY-like interaction, there are difficulties in using such an approach to explain all of the experimental results. This is in part due to the fact that more accurate calculations of the conduction electron susceptibilities of the rare earths are needed before it can be judged finally whether or not this type of approach provides an adequate description. A more profound difficulty is that a
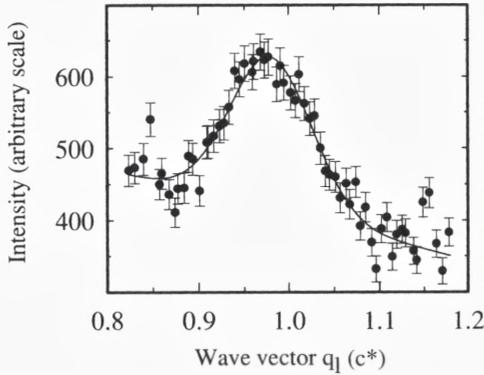
Figure 10. Representative scan along the $c^*$ direction through the magnetic reflections in Nd/Pr from the cubic sites. The scan direction was along $q_l$ through $(q_h^{cubic} \, 0 \, q_l)$ with $q_h^{cubic} \approx 0.19$ r.l.u. (Goff et al., 1996).

full description of the magnetic interactions in the rare earth superlattices requires due consideration of the localised $4f$ electrons (single-ion anisotropy, etc) as well as the nature of the conduction electron states in a superlattice. This remains a formidable challenge.

# Acknowledgements

# References

Baibich MN, Broto JM, Fert A, Nguyen Van Dau F and Petroff F, 1988: Phys. Rev. Lett. **61**, 2472

Bryn-Jacobsen C, Cowley RA, McMorrow DF, Goff JP, Ward RCC and Wells MR, 1997: Phys. Rev. B (In press)

Beach RS, Borchers JA, Erwin RW, Flynn CP, Mathney A, Rhyne JJ and Salamon MB, 1992: J. Magn. Magn. Mater. **104-107**, 1915

Bjerrum Møller H, Jensen JZ, Wulff M, Mackintosh AR, McMasters OD and Geschneider Jr. KA, 1982: Phys. Rev. Lett. **49**, 482

Dumesnil K, Dufour C, Vergnat M, Marchal G, Mangin P, Hennion M, Lee WT, Kaiser H and Rhyne JJ, 1994: Phys. Rev. B **49**, 12274

Erwin RW, Rhyne JJ, Salamon MB, Borchers JA, Sinha S, Du R, Cunningham JE and Flynn CP, 1987: Phys. Rev. B **35**, 6808

Everitt BA, Borchers JA, Salamon MB, Rhyne JJ, Erwin RW, Park BJ and Flynn CP, 1995: J. Magn. Magn. Mater. **144**, 769

Goff JP, Bryn-Jacobsen C, McMorrow DF, Ward RCC and Wells MR, 1996: J. Magn. Magn. Mater. **156**, 263

Jehan DA, McMorrow DF, Cowley RA, Wells MR, Ward RCC, Hagman N and Clausen KN, 1993: Phys. Rev. B **48**, 5594

Jensen J and Mackintosh AR, 1991: *Rare Earth Magnetism: Structures and Excitations* (Clarendon Press, Oxford)

Koehler WC, Cable JW, Wilkinson MK and Wollan FO, 1966: Phys. Rev. **151**, 414

Kwo J, Gyorgy EM, McWhan DB, Disalvo FJ, Vettier C, and Bower JE, 1985: Phys. Rev. Lett. **55**, 1402

Kwo J, 1987: *Thin Film Growth Techniques For Low Dimensional Structures*, eds. R.F.C. Farrow, S.P. Parkin, P.J. Dobson, J.H. Neave and A. Arrott (Plenum, London)

Liu SH, Gupta RP and Sinha SK, 1971: Phys. Rev. B **4**, 1100

Majkrzak CF, Cable JW, Kwo J, Hong M, McWhan DB, Yafet Y, Waszczak JV, Grimm H and Vettier C, 1986: Phys. Rev. Lett. **56**, 2700

Majkrzak CF, Kwo J, Hong M, Yafet Y, Gibbs D, Chien CL and Bohr J, 1991: Adv. Phys. **40**, 99

McEwen KA and Stirling WG, 1981: J. Phys. C **14**, 157

McMorrow DF, Swaddling PP, Cowley RA, Ward RCC and Wells MR, 1996: J. Phys. Condens. Matter **8**, 6553

Moon RM, Cable JW and Koehler WC, 1964: J. Appl. Phys. **35**, 1041

Rhyne JJ and Erwin RW, 1993: *Magnetism in Aritificial Metallic Superlattices of Rare Earth Metals*, in Magnetic Materials **8**, ed. K.H.J. Buschow

Salamon MB, Sinha S, Rhyne JJ, Cunningham JE, Erwin RW, Borchers J and Flynn CP, 1986: Phys. Rev. Lett. **56**, 259

Simpson JA, McMorrow DF, Cowley RA, Jehan DA, Wells MR, Ward RCC and Clausen KN, 1994: Phys. Rev. Lett. **73** 1162

Simpson JA, McMorrow DF, Cowley RA, Wells MR and Ward RCC, 1995: J. Phys. Condens. Matter **7**, L417

Simpson JA, Cowley RA, McMorrow DF, Ward RCC and Wells MR, 1996: J. Phys. Condens. Matter **8**, L187

Swaddling PP, McMorrow DF, Simpson JA, Wells MR, Ward RCC and Clausen KN, 1993: J. Phys. Condens. Matter **5**, L481

Swaddling PP, Cowley RA, Wells MR, Ward RCC and McMorrow DF, 1996: Phys. Rev. B **53**, 6488

Tsui F, Flynn CP, Beach RS, Borchers JA, Erwin RW and Rhyne JJ, 1993: J. Appl. Phys. **73**, 6904

Yafet Y, Kwo J, Hong M, Majkrzak CF and O'Brien T, 1988: J. Appl. Phys. **63**, 3453

Wilkinson MK, Koehler WC, Wollan EO and Cable JW, 1961: J. Appl. Phys. **32**, 48S